13th World Conference on Earthquake Engineering
Vancouver, B.C., Canada
August 1-6, 2004
Paper No. 930

NUMERICAL SIMULATION OF HIGH-RISE STEEL BUILDINGS USING IMPROVED APPLIED ELEMENT METHOD

Said ELKHOLY[1] and Kimiro MEGURO[2]

SUMMARY

This work addresses the field of collapse analysis of steel framed structures under severed loading conditions. Applied Element Method (AEM) is recognized as a powerful tool for analyzing the structural behavior from the early stage of loading up to total collapse. This method has been used successfully with different types of material such as reinforced concrete, soil and masonry. A new extension of this method is proposed in this paper in order to simulate large-scale steel structures. The Improved Applied Element Method (IAEM) has been presented and employed in the development of novel numerical solutions for analysis of failure and collapse of large-scale structures under different hazardous loads. A series of numerical examples, including both geometric and material nonlinearity, are used for validation of the improved method. The results indicate that the improved method is capable of accurately analyzing the ultimate load-carrying capacity of steel structures. The case study, presented in this paper, shows different collapse mechanisms of a moment resistance steel frame structure under severe ground motions.

INTRODUCTION

The 1994 U.S Northridge earthquake caused serious damage to modern steel structures. The brittle fractures of beam-to-column connections for the moment frame building were widely observed [1;2]. The damaged buildings were of various heights ranging from one story to 26 stories. One year later, in the Kobe earthquake (1995), nearly one thousand steel buildings were damaged, as well as 90 buildings being collapsed, 333 buildings being severely damaged, and 300 being slightly damaged [3;4]. According to the FEMA report, modern steel-frame buildings, specially constructed to sway rather than fracture during an earthquake, are more vulnerable to collapse than had ever been considered. A design flaw could cause these often massive skyscrapers to crack, tilt and even collapse during violent shaking [2]. To reduce such damage, it is important to understand its main mechanism. However, it is very difficult or practically impossible to perform damage tests for total collapse process of real scale steel structures, especially high rise buildings. Therefore, studying those phenomena requires powerful numerical tools that can extend the analysis up to complete failure.

To obtain full knowledge of the behavior of steel structures under severe ground motions, the current research is aimed at establishing a comprehensive numerical technique to evaluate and characterize the

1 Ph. D Candidate, The University of Tokyo, 4-6-1 Komaba, Meguro-ku, Tokyo 153-8505, Japan
2 Associate Professor, Institute of Industrial Science, The University of Tokyo, Japan

earthquake response as well as the characteristics and failure mechanisms of large-scale structures. The emphasis is placed on the collapse mechanisms and the associated behavior of structures and their members under large cyclic loading. During the last decades, considerable research effort dealing with collapse analysis has been developed such as Rigid Bodies Spring Model (RBSM) [5], Extended Distinct Element Method (EDEM) [6], combined FEM/DEM [7], and Applied Element Method (AEM) [8-12]. Nevertheless, none of them have yet been used for collapse analysis of steel structures. In order to guarantee decent accuracy of the solution in the case of modeling of steel structure using AEM, a very large number of elements will be required to extend the computer power and time needed for numerical simulation. Therefore, this paper describes the methodology of Improved Applied Element Method (IAEM) [13,14], an efficient and accurate method for analyzing the failure and collapse of large-scale structures under hazardous loads.

In this paper, the formulations of IAEM are presented, where the effects of geometric and material nonlinearities are considered. The main features and analysis capabilities of IAEM are discussed, and verification examples are performed to demonstrate the extreme efficiency of the developed code in performing inelastic analysis for steel structures. The IAEM requires a very small number of degrees of freedom compared to conventional AEM, while decreasing the CPU time needed for analysis and increasing the capacity of the solver. A case study shows the different collapse mechanisms of a nine-story steel structure model under severe ground motion excitation. The proposed method can be utilized to achieve better understanding of the response of structures toward ground motion, impact, fire, and hazardous blasting.

INTRODUCTION TO APPLIED ELEMENT METHOD

Applied Element Method (AEM), Ref. [6-10], is a recently developed method for structural analysis in both small and large displacement ranges. This method can follow the structural behavior since the application of load, crack initiation and propagation, separation of structural elements and until total collapse can be done in a reasonable time with reliable accuracy. In AEM, a given structure is divided into a proper number of rigid body elements. A pair of elements is connected with pairs of normal and shear springs uniformly distributed on the boundary line. Each pair of springs represents total stresses and deformations of a certain area (hatched area in **Fig.1**) of the studied elements. Therefore, the normal and shear stiffness can be determined by Eq. (1).

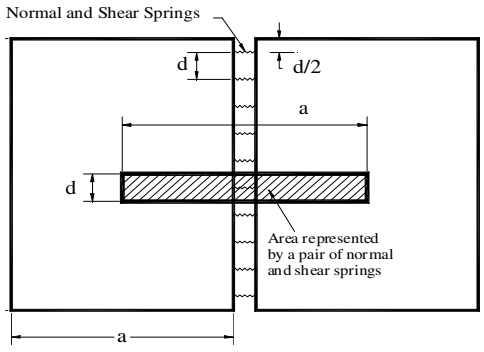

Figure 1: Area of influence of each pair of springs

$$K_n = \frac{E*d*T}{a} \quad \text{and} \quad K_s = \frac{G*d*T}{a} \tag{1}$$

where d is the distance between each spring; a is the length of the representative area; E and G are Young's and shear modules of the material, respectively; and T is the thickness of the element, which is considered constant for all springs attached to the element [8].

Although the conventional AEM used in different engineering fields had shown high accuracy and applicability like reinforced concrete [10], soil [11] and masonry [12], some other applications however are difficult to handle, such as huge steel structure buildings. Using the current version of AEM, elements with a very small size should be used to follow the change in the thickness especially in non-rectangular cross sections (i.e. I Shape, Channel, and Boxed sections), since the element should be chosen to fit the flange thickness. In this paper, we introduce the Improved Applied Element Method which can easily handle the aforementioned cases.

IMPROVED APPLIED ELEMENT METHOD

Modification of spring stiffness

Two major extensions of the AEM have been implemented: The first is that of improving the element type to be able to follow any change in the non-rectangular cross-section thickness. the second is that allowing different thicknesses to be used for calculating normal stiffness and shear stiffness. This sort of modification allows using large elements, having the same cross sectional geometric parameters as normal and shear and bending stiffness. The value of normal and shear stiffness for each pair of springs can be determined by Eq. (2).

$$K_n^i = \frac{E \cdot d \cdot T_n^i}{a} \quad \text{And} \quad K_s^i = \frac{G \cdot d \cdot T_s^i}{a} \tag{2}$$

where: T_n^i and T_s^i are the thickness represented by the pair of springs "*i*" for normal and shear cases, respectively. This difference in the value of T_n^i and T_s^i owes to the change in effective area for both normal and shear directions

A pair of rigid elements, as shown in **Fig. 2**, are assumed to be connected by only one pair of normal spring stiffness (K_n^i) and shear spring stiffness (K_s^i). The values of dx and dy correspond to the relative coordinate of the contact point with respect to the center of gravity. To have a global stiffness matrix, the location of elements and contact springs is assumed in a general position. The stiffness matrix components corresponding to each D.O.F. are determined by assuming a unit displacement in the studied direction and by determining forces at the centroid of each element. The element stiffness matrix size is only (6 x 6). Eq. 3 shows the components of the upper left quarter of the stiffness matrix. All notations used in this equation are shown in **Fig. 2**.

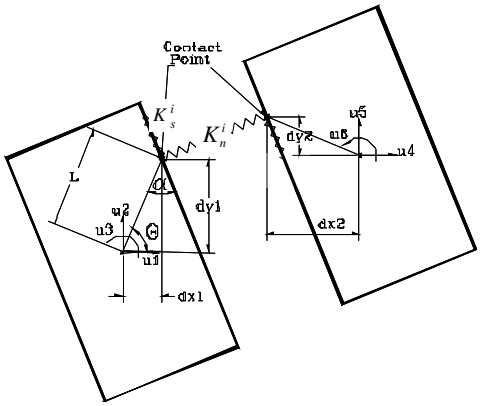

Figure 2: Contact Point and D.O.F

$$\begin{bmatrix} Sin^2(\theta+\alpha)K_n^i & -K_n^i Sin(\theta+\alpha)Cos(\theta+\alpha) & Cos(\theta+\alpha)K_S^i LSin(\alpha) \\ +Cos^2(\theta+\alpha)K_S^i & +K_S^i Sin(\theta+\alpha)Cos(\theta+\alpha) & -Sin(\theta+\alpha)K_n^i LCos(\alpha) \\ -K_n^i Sin(\theta+\alpha)Cos(\theta+\alpha) & Sin^2(\theta+\alpha)K_S^i & Cos(\theta+\alpha)K_n^i LCos(\alpha) \\ +K_S^i Sin(\theta+\alpha)Cos(\theta+\alpha) & +Cos^2(\theta+\alpha)K_n^i & +Sin(\theta+\alpha)K_S^i LSin(\alpha) \\ Cos(\theta+\alpha)K_S^i LSin(\alpha) & Cos(\theta+\alpha)K_n^i LCos(\alpha) & L^2Cos^2(\alpha)K_n \\ -Sin(\theta+\alpha)K_n^i LCos(\alpha) & +Sin(\theta+\alpha)K_S^i LSin(\alpha) & +L^2Sin^2(\alpha)K_S^i \end{bmatrix} \tag{3}$$

Although in this method, we can change the characteristics of all springs surrounding any element, in practice, only changing the corner springs is needed for steel flanged sections. As shown in **Fig. 3**, changing the ratios of (K_1/K_2) and (K_3/K_4) can control the stiffness of any element. That kind of improvement allows using many different flanged steel sections like I-beam, Box and Channel cross sections. Moreover, any cross section can be simulated by adjusting the values of the element height, number of springs, ratio of outer to inner thickness, and the ratio of normal to shear thickness.

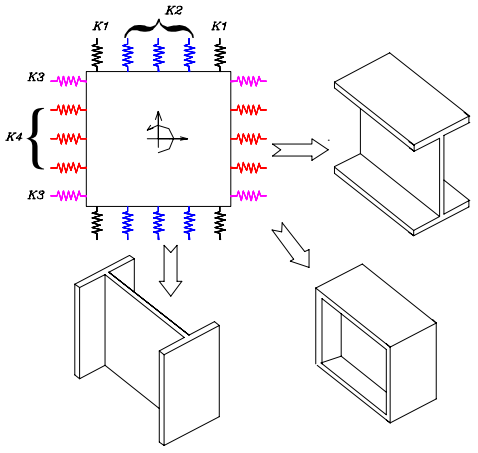

Figure 3: Element Shape for IAEM

Modification in dynamic properties

The general differential equation of motion, governing the response of structure in a small displacement range can be expressed as:

$$[M]\{\Delta\ddot{U}\}+[C]\{\Delta\dot{U}\}+[K]\{\Delta U\}=\Delta f(t)-[M]\{\Delta\ddot{U}_G\} \quad (4)$$

where: [M] is mass matrix; [C] is the damping matrix; [K] is the nonlinear stiffness matrix; Δf(t) is the incremental applied load vector; $\{\Delta\ddot{U}\},\{\Delta\dot{U}\},\{\Delta U\}$ and $\{\Delta\ddot{U}_G\}$ are the incremental acceleration, velocity, acceleration, and gravity acceleration vectors, respectively.

In IAEM, the mass matrix and the polar moment of inertia of each element have been idealized as lumped at the element centroid. The corresponding lumped mass in each DOF direction can be calculated by summing the effect of small segmental masses represented by each spring considering the change of the springs' thickness. Eq. (5) represents the value of lumped mass in each degree of freedom direction assuming that elements are square in shape.

$$\begin{bmatrix} M1 \\ M2 \\ M3 \end{bmatrix} = \begin{bmatrix} \frac{D^2\cdot\rho}{nsp}\cdot\sum_{i=1}^{i=nsp} t_i^x \\ \frac{D^2\cdot\rho}{nsp}\cdot\sum_{i=1}^{i=nsp} t_i^y \\ \frac{D^4\cdot\rho}{nsp}\cdot\sum_{i=1}^{i=nsp}\left(\frac{t_i^x}{12}+\frac{t_i^y}{12}\right) \end{bmatrix} = \begin{bmatrix} D^2\cdot\rho\cdot t_{av} \\ D^2\cdot\rho\cdot t_{av} \\ \frac{D^4\cdot\rho}{nsp}\cdot\sum_{i=1}^{i=nsp}\left(\frac{t_i^x}{12}+\frac{t_i^y}{12}\right) \end{bmatrix} \quad (5)$$

where: D is the element size; t_{av} is the average thickness of the element; ρ the density of the material considered. It should be noticed that the $[M_1]$ and $[M_2]$ are corresponding to the element mass and $[M_3]$ is corresponding to the element polar moment of inertia about the center of gravity.

Large displacement analysis with Improved AEM

The concept of large displacement analysis has been introduced by Tagel-Din [9]. According to their concept, the AEM can follow the large deformation under both static and dynamic load by applying a slight change in the equation of motion **Eq. 6**.

$$[M]\{\Delta\ddot{U}\}+[C]\{\Delta\dot{U}\}+[K]\{\Delta U\}=\Delta f(t)+R_m+R_G \quad (6)$$

where R_m represents the residual force vector due to cracking and incompatibility between strain and stress of each spring; and R_G the residual force vector due to geometrical changes in the structure during loading.

By assuming R_m and R_G equal to null and solving **Eq. 6** to get ΔU, the structural geometry can be modified according to the calculated incremental displacements. According to the modification of geometry of structure and checking the occurrence of cracks, new values for R_m and R_G can be calculated. By using new values of R_m and R_G to recalculate the incremental displacement ΔU, considering the stiffness changes due to cracking and yielding, analyzing the structure subjected to dynamic loading can allow us to follow both geometrical changes of the structure and rigid body motion during failure.

The validity of the developed code had been demonstrated by several numerical examples. The verification examples indicate that IAEM shows excellent agreement with both theoretical and finite element results in linear static and dynamic load conditions [13,14].

Material modeling

Insofar, a simplified uniaxial bilinear stress-strain model with kinematic strain hardening is adapted for representing the normal stiffness component of structural steel, as shown in **Fig. 4**. In this model the plastic range remains constant throughout the various loading stages, and the kinematic hardening rule for the yield surface is assumed as a linear function of the

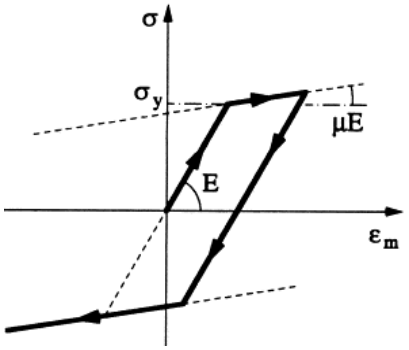

Figure 4: Bilinear Material Model

increment of plastic strain. In this model, the strain hardening parameter (μ) is represented as the ratio between the post-yield stiffness (E_{sp}) and the initial elastic stiffness (E_y) of the material. The former is defined as **Eq.** (8).

$$E_{sp}=(F_{ult}-F_y)/(\varepsilon_{ult}-\varepsilon_y) \quad (8)$$

where F_{ult} and ε_{ult} represent the ultimate or maximum stress and strain capacity of the material, respectively. Although, this is not an entirely realistic representation of the material behavior, it allows for the hardening to be included whilst keeping the formulation simple

INELASTIC ANALYSIS FOR STEEL STRUCTURES

Introduction

Over the past decades, numerous researchers have developed and validated various methods of performing the inelastic analysis on steel frames based on second order inelastic analysis which can be categorized into two main types: (1) plastic zone (2) plastic hinge based approach.

The Elastic–plastic analysis is considered the most direct and simplified approach for representing the material nonlinearity. In this model the element is assumed to remain elastic except at the places where zero length plastic hinges are allowed to form Giberson [15], Chen[16]. This method accounts for inelasticity but it can't account for the spread of yielding through the section. Therefore, it is not possible to capture member stability with enough accuracy for a wide range of beam-to-column problems [17].

Plastic zone analysis: in which the spread-of-plasticity of the member is assumed to be modeled by subdividing the frame members into several finite elements. Furthermore, each element is subdivided into many fibers [18-19]. The plastic zone solution is known as an exact solution. This method has been used in IAEM whereas the connecting springs work as fibers. Once the strain of each spring is calculated, the stress state can be explicitly determined and the gradual spread of yielding traced.

Two examples are presented hereafter to demonstrate that the proposed IAEM for carrying out an elasto plastic analysis for structures is efficient and accurate.

Illustrative examples and results

Example 1: The ultimate long span steel beam

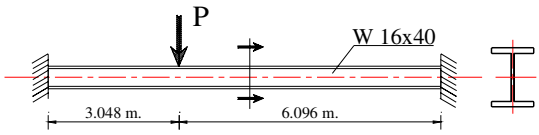

Figure 5: Long-span steel beam

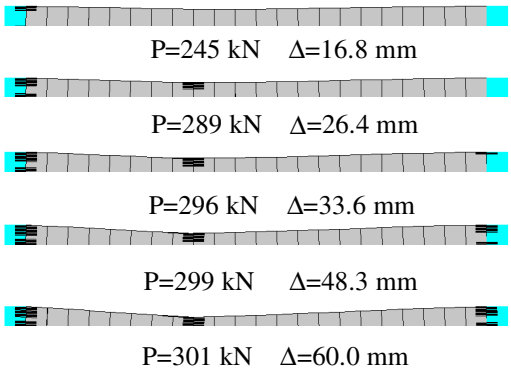

Figure 6: Formation of plastic zones

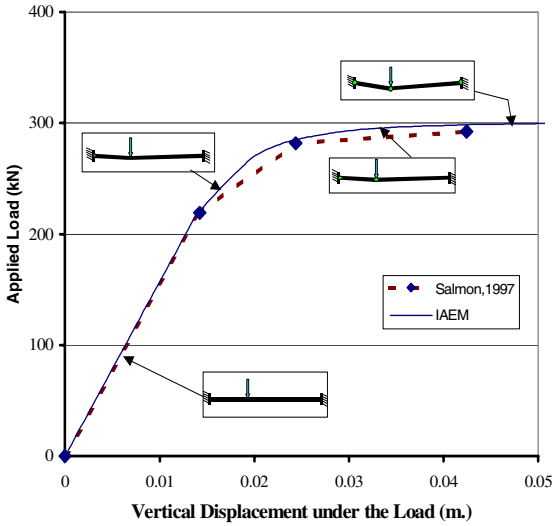

Figure 7: Ultimate load carrying capacity of a plane steel beam

The first example is a 16x40 wide flange section steel beam of 9.14 m span. The dimensions, supports, loading conditions, and cross section are shown in **Fig. 5**. The beam has a modulus of elasticity of

205GPa and yield strength of 248MPa. The beam is loaded at one-third points along its span. With the IAEM, 24 general shaped elements are used including two boundary elements. However, 22357 square elements with a constant thickness are required to model the same beam using original AEM while taking in consideration the variation in thickness for flanges and web. Based on IAEM analysis, the sequences plastic collapse mechanism of the beam and the formation of the plastic zones are shown in **Fig. 6**.The results obtained by the proposed method (IAEM) are compared with those by Salmon [20]. The results are presented in vertical load versus deflection at the loaded point curve as shown in **Fig. 7**. The comparison shows a very good agreement with the theoretical results.

Example 2. The ultimate load-carrying capacity of plane steel frame

The second example of the ultimate carrying load capacity analysis, which has been taken from Ren [22], is that of a rectangular portal frame with rigid connections and a fixed base, as shown in **Fig. 8.** The frame is divided into 61 rigid elements. The cross section and material properties of the members are listed in **Table 1**. The horizontal and vertical loads are applied as shown in **Fig. 8.** The ultimate load capacity of the frame, according the experimental test that was carried out by Hodge [21] was 133.0kN. However, based on IAEM, the maximum frame resistance is reached at load (P) of 136kN which is around 2% higher than the maximum recorded load during the experiment. The load-vertical displacement curve obtained by both IAEM and the Rigid Body-Spring discrete element Method (RBSM) obtained by Ren [22] are plotted in **Fig. 9** as well as the experimental data by Hodge [21]. **Fig. 10** shows the location of the developed plastic zones which are represented as dark areas in the figure. The results demonstrate the good agreement with experimental and RBSM results.

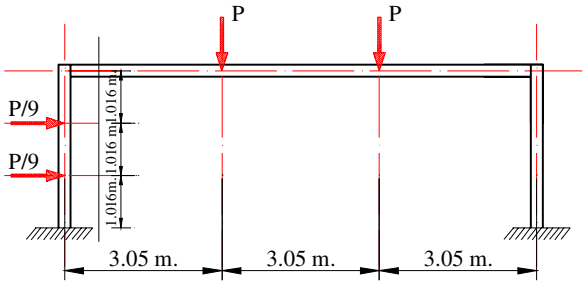

Figure 8: Analysis Model

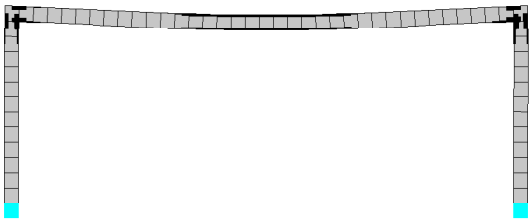

Figure 10: Location of plastic hinges

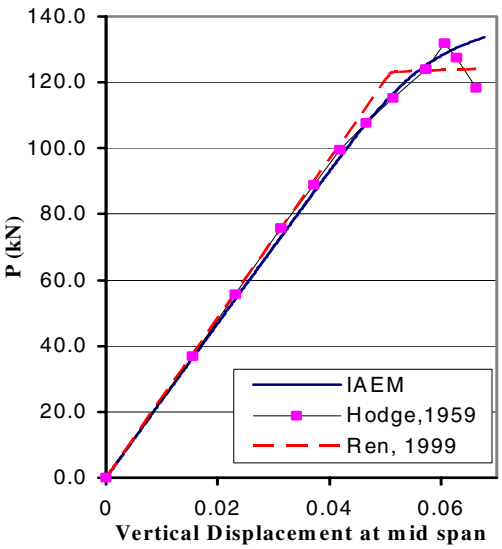

Figure 9: Ultimate load carrying capacity of a plane steel frame

Table 1: Cross-section and material properties of members

Area (m^2)	Inertia (m^4)	E (kN/mm^2)	Fy (N/mm^2)	Poisson's ratio
0.6448×10^{-2}	1.08856×10^{6}	209	275.8	0.3

CASE STUDY - COLLAPSE OF A NINE-STORY STEEL BUILDING

One of the main advantages of the analytical method is its versatility in parametric study of collapse cases. In this section, the IAEM is applied to investigate the validity of the proposed method in simulating

progressive failure of steel structural buildings under hazardous load conditions, the collapsing process of a multi-story steel structure under severe ground motion conditions is presented in this section. The structure considered is a plane nine-story steel frame with three bays of 9.00m long, as illustrated in **Fig. 11**. The typical height per story is 3.75m. The dimensions of the structural members are given in **Table 2**. in this frame, columns are bent about their major axes and rigid connections are assumed. The building was designed in accordance with the 1997 NEHRP recommended seismic provisions [23]. Young's modulus is taken as 205GPa and yield stress is 275 MPa and 355 MPa for beams and columns, respectively. Rayleigh damping with 5% damping for the first fundamental mode was assumed. Using IAEM, only 477 elements are utilized for modeling the whole structure.

Table 2 Cross sections assigned for a 9-story steel building

Columns			Beam
Story	Exterior	Interior	
9	w14x342	w14x398	w21x62
8	w14x342	w14x398	w27x94
7	w14x398	w14x455	w33x118
6	w14x398	w14x455	w33x118
5	w14x455	w14x550	w36x150
4	w14x455	w14x550	w36x150
3	w14x455	w14x550	w36x150
2	w14x550	w14x550	w40x183
1	w14x550	w14x605	w40x183

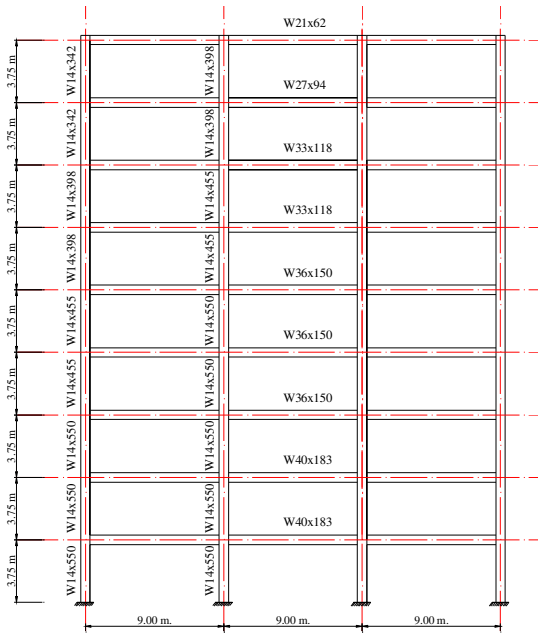

Figure 11: Nine-story steel frame

Seismic response

The inelastic dynamic analysis has been performed, which integrates step-by-step the differential equations of motion corresponding to a given seismic input. Both material and geometric nonlinearity has been considered. Displacement time history analysis has been conducted of combined horizontal and vertical components of the first 40 seconds of the Hyogoken-Nanbu Earthquake (1995). The PGA of the horizontal component (KOBE/KJM000) was 813gal and had a PGD of 17.68cm while the vertical component (KOBE/KJM-UP) had a peak ground acceleration of 336gal and a PGD of 10.29cm.

Collapse analysis

This paper illustrates a simulation of the building collapse under two different failure modes. The first failure is ground floor type failure as illustrated in **Fig. 12**. A reduction of 40 % of steel strength of the columns at ground level and lack of ductility in column-to-beam connections were assumed. The intense shaking caused the failure of load bearing columns in the lower floor level and cause progressive failure. According to the figure, firstly the ground motion excitation resulted in the formation of plastic hinges at several locations. The zones that have plastic deformation are represented by dark color in the figure. From the figure, it can be noted that most of the plastic hinges formed in beams, instated of columns, is due to the strong column-weak beam design philosophy. With the progress of time and formation of enough plastic hinges, the weakness of the strength and the low ductility demand of the ground floor level produced a failure in the ground floor columns. The end stage of the failure, illustrated in **Fig. 12**, shows a good agreement with a recorded collapse case of multi-story steel buildings due to Hyogoken-Nanbu, Kobe Earthquake (1995) (as shown in **Fig. 13).**

Another well observed failure mode is the intermediate soft floor type of failure. This failure mechanism had been widely observed for many multi-story steel buildings due to Kobe Earthquake (1995), as illustrated in **Fig. 14**. The sequence of intermediate soft-story failure based on IAEM simulation is

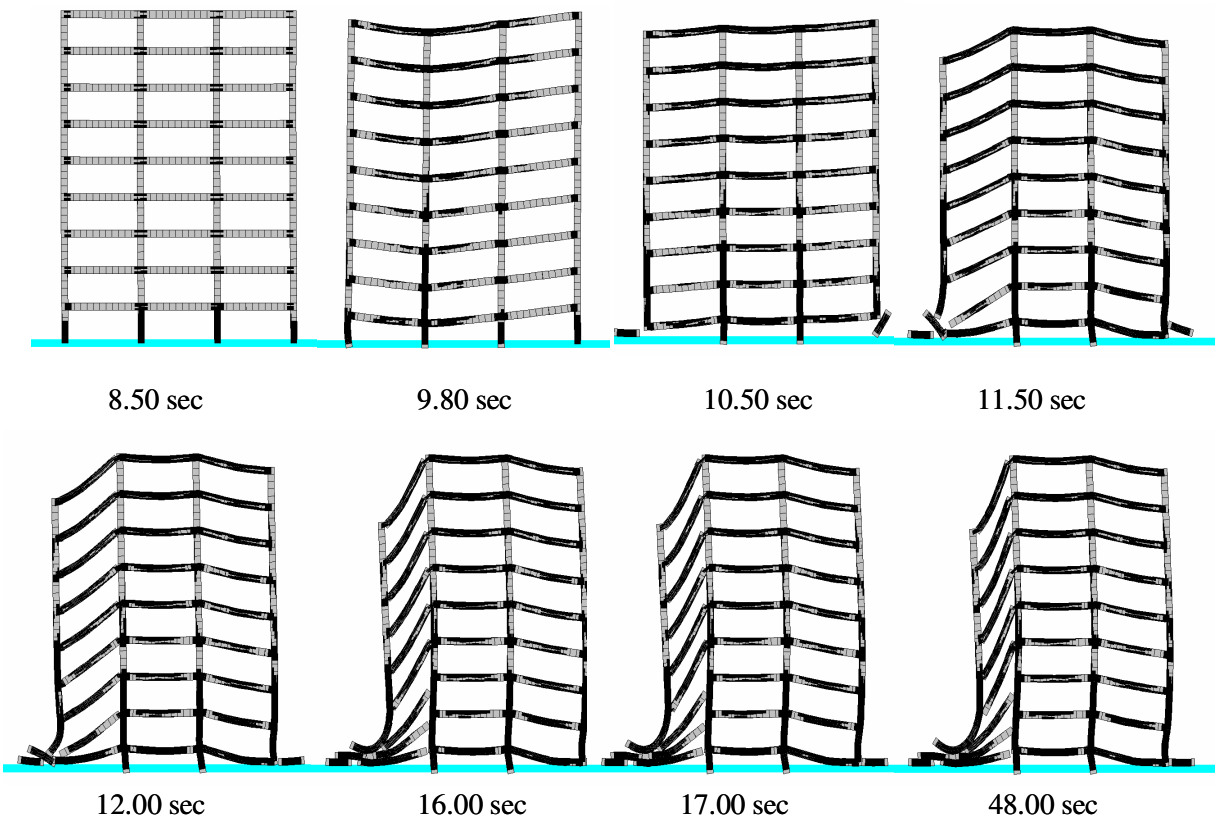

Figure 12: *Ground soft-story collapse mechanism*

Figure 13: *Collapsed steel building during January 17,1995 Kobe Earthquake (by K. Meguro)*

(by K. Meguro)

Figure 14: Collapsed commercial buildings during January 17, 1995 Kobe Earthquake

illustrated in **Fig. 15**.The collapse had been initiated due to the same assumption of weakness of columns and reduction of ductility at intermediate floor level. The weakness of columns and the intensity of the ground motion develop inelastic behavior through the formation of yielding zones at the connections between beams and columns. Developing plastic zone hinges permit free lateral displacement of frame to occur and initiate the failure.

From the results, it can be concluded that the collapse of large scale structures due to earthquakes can be performed with sufficient accuracy by using the well-verified and calibrated analysis tool (IAEM). The calculation time required for the simulation of complete failure required only approximately one and half hours on a personal computer. This was due to the simplification of the IAEM which assumes much fewer number of elements compared to traditional methods. Such a minimal requirement of computational time, with acceptable accuracy, can be considered as a unique advantage of this model.

CONCLUSIONS

This paper has attempted to briefly trace the development of the IAEM for analyzing the entire behavior of large scale steel structures up to total failure. The main feature of this tool is to use as few elements as possible to model each structural component and to obtain a realistic representation of material and geometric non-linearity. The tool was used to analyze available numerical and experimental cases to verify the accuracy of the improved method. The results indicate that the improved method is capable of accurately analyzing the ultimate load-carrying capacity of steel structures. Numerical examples showing the accuracy, efficiency, and the range of application are presented. The program is a

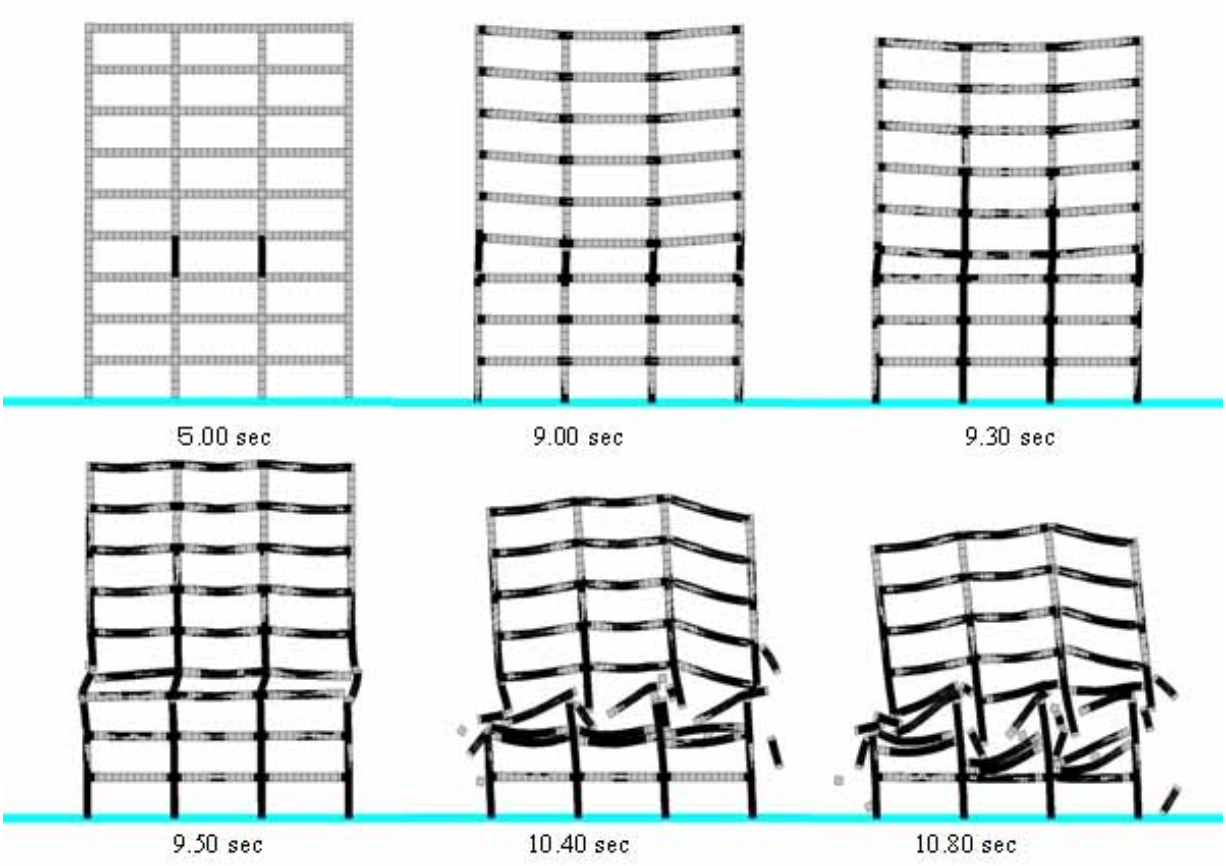

Figure 15: Sequences of soft-story failure of multi-story steel framed structure

useful tool for performing intensive parametric studies to achieve a deeper understanding of structural behavior of steel structures under strong ground motions. Our method can help engineers to investigate the performance of even high-rise buildings under different hazardous loads. The mechanism of progressive failure and the effect on the neighboring buildings can also be simulated.

The proposed method is limited to two dimensional frames composed of members with compact sections, fully braced out-of plane. The section of members can develop full plastic moment capacity without occurrence of lateral tortional buckling. More research work is needed to extend the capability of the numerical technique to capture the details of inelastic behavior associated with lateral tortional buckling and local buckling.

REFERENCES

1. Miller D. K. "Lessons learned from the Northridge earthquake, Engineering Structures." J. Eng. Struct. 1998, 20(4-6): pp 249-260
2. FEMA. Recommended seismic design Criteria for New Steel Moment-Frame Buildings, Report No. FEMA 350, FEMA, Washington, DC, 2000
3. Nakashima M., Inoue K., and Tada M. "Classification of Damage to Steel Buildings Observed in the 1995 Hyogoken-Nanbu Earthquake", Eng. Struct. 1998, 20(4-6): 271-281
4. Holguin R., Building Department's Response to EQ Damage to Steel Frame Buildings. Journal of Performance of Constructed Facilities 1998; 12(4): 199–201.
5. Toi, Y. and Yoshida, S., "Numerical Simulation of Nonlinear Behaviors of Two-Dimensional Block Structures." Computers and Structures 1991; 41(4): 593-603.

6. Meguro, K., Iwashita, K., and Hakuno, M. “Fracture Analyses of Structures by the Modified Distinct Element Method.” Struct. Engrg./Earthquake Engrg 1991; 6(2): 283–294.
7. Munjiza, A., Owen, D. R. J., and Bicanic, N. “A Combined Finite-Discrete Element method in Transient Dynamic of Fracturing Solids.” Engineering Computations 1995, 12: 145-174.
8. Meguro, k. and Tagel-Din, H. “Applied Element Simulation of RC Structures under Cyclic Loading.” ASCE 2001, 127(11): 1295-1305.
9. Tagel-Din, H. and Meguro, K. “Applied Element Method for Dynamic Large Deformation Analysis of Structures.” Structural Eng./Earthquake Eng., JSCE2000, 17(2): 215-224.
10. Tagel-Din, H. and Meguro, K. “Analysis of a Small Scale RC Building Subjected to Shaking Table Tests using Applied Element Method.” Proceedings of the 12th WC EE 2000, New Zealand.
11. Ramanchara, P. ・ Meguro K. “Nonlinear Static Modeling of Disp-Slip Fault for Studying Ground Surface Deformation using Applied Element Method,” Structural Eng./Earthquake Eng., JSCE 2002, 9(2): 169-178.
12. Mayorca, P. and Meguro K. “Extension of the Applied Element Method for the Analysis of Masonry Structures.” Proceedings 4th International Summer Symposium 2002, JSCE: 41-44.
13. Elkholy, S. and Meguro K. “Dynamic Progressive collapse of High-Rise Buildings”, the 2nd International Symposium on New Technologies for Urban Safety of Mega Cities in Asia 2003, Tokyo, Japan: 323-330.
14. Elkholy, S., Tagel-Din, H., and Meguro k.: “Structural Failure Simulation due to Fire by Applied Element Method”, The Fifth Japan Conference on Structural Safety and Reliability, JCOSSAR 2003:47-52.
15. Giberson, M. F. “Two Nonlinear Beams with Definitions Ductility” J. Struct. Div., ASCE 1969. vol. 95 (ST2): 137-157.
16. Chen WF, Goto Y, Liew JYR. “Stability Design of Semi-Rigid Frames”. Wiley: New York, 1996
17. Liew JYR, White DW, Chen WF. “Second-order refined plastic hinge analysis for frame design: parts 1 and 2.” J struct. Eng. ASCE 1993; vol. 119, No. 11, 3196-3237
18. Chan SL. “Inelastic post-buckling analysis of tubular beam-columns and frames,” J. Eng. Struct. 1989;11:23–30.
19. Clarke MJ. “Plastic zone analysis of frames.” In: Chen WF, Toma S, editors. Advanced analysis of steel frames. Boca Raton, FL: CRC Press; 1994.
20. Salmon CG, and Johnson H. “Steel structures – design and behavior”, Addison-Wesley Pub, 4th edition,1997, ISBN: 0673997863
21. Hodge Jr PG. “Plastic analysis of structures,” New York: McGraw-Hill, 1959
22. Ren W., Tan X. and Zheng Z. “Nonlinear analysis of plane frames using rigid body-spring discrete element method”, Computers & Structures, 1999, 71(1), pp105-119
23. Foutch, DA. And Yun SY. “Modeling of Steel Moment Frames for seismic loads,” J. of Constructional Steel Research 2002, 58(5-8):529-564